

# On the Polymorphism of White Phosphorus<sup>☆</sup>

Arndt Simon\*, Horst Borrmann, and Jörg Horakh

Max-Planck-Institut für Festkörperforschung,  
Heisenbergstraße 1, D-70569 Stuttgart, Germany  
Fax: (internat.) +49(0)711/689-1642

Received April 16, 1997

**Keywords:** Phosphorus / Phase transitions / Molecular crystal / Crystal growth / Low-temperature crystal structure / Librational motion

White phosphorus occurs in three modifications. The  $\alpha$  form, which exists at room temperature, transforms reversibly to the  $\beta$  form at  $-77^\circ\text{C}$ . The  $\alpha \rightarrow \beta$  transformation may be strongly delayed. Quenching the  $\alpha$  form to  $-185^\circ\text{C}$  followed by slow warming results in an exothermic reaction with formation of the  $\gamma$  form which transforms into the  $\beta$  form at  $-120^\circ\text{C}$  in an endothermic reaction. A transition  $\beta \rightarrow \gamma$  is not observed. The  $\gamma$  form is characterized by its powder diagram. The structure of the  $\beta$  form is redetermined from a single

crystal at  $-185^\circ\text{C}$  ( $P\bar{1}$ ,  $a = 547.88(5)$ ,  $b = 1078.62(11)$ ,  $c = 1096.16(11)$  pm,  $\alpha = 94.285(8)$ ,  $\beta = 99.653(7)$ ,  $\gamma = 100.680(7)^\circ$ ,  $V = 623.79(10) \cdot 10^6$  pm<sup>3</sup>,  $Z = 6$  formula units per cell). The  $P_4$  molecules exhibit pronounced librational motion in spite of the low temperature of investigation. The arrangement of the centers of the tetrahedra corresponds to the atom positions in the  $\gamma$ -plutonium structure, which is discussed in relation to the  $bcc$  structure.

Liquid and gaseous phosphorus consists of  $P_4$  molecules which start to decompose into  $P_2$  molecules above  $800^\circ\text{C}$ <sup>[1]</sup>. The most reactive allotropic modification, "white" phosphorus, forms from the gas phase. At room temperature  $\alpha$ - $P_4$  is a plastic crystal<sup>[\*]</sup>.

Bridgman<sup>[2]</sup> discovered a reversible phase transition into  $\beta$ - $P_4$  which is formed below  $-77^\circ\text{C}$  at ambient pressure or under 10 kbar pressure at room temperature. When investigating the temperature dependence of spin-lattice relaxation times of white phosphorus, Spiess, Grosescu and Haeberlen<sup>[3]</sup> found indications for the existence of a third modification ( $\gamma$ - $P_4$ ) which forms – sometimes only within hours – when  $\alpha$ - $P_4$  is quenched to  $-165^\circ\text{C}$  and kept at that temperature.  $\gamma$ - $P_4$  transforms into the  $\beta$  modification when warmed to  $-115^\circ\text{C}$ , without a chance to recover  $\gamma$ - $P_4$  by cooling the sample again.

Early X-ray investigations on  $\alpha$ - $P_4$  suffered from its partial transition into red phosphorus<sup>[4–6]</sup>. From single-crystal investigations at  $-30^\circ\text{C}$  the most probable space group  $I\bar{4}3m$  with  $a = 1851(3)$  pm was derived<sup>[7]</sup>. The proposed structural relationship with  $\alpha$ -Mn<sup>[8–10]</sup> –  $P_4$  molecules taking the positions of the metal atoms – could later be verified<sup>[11]</sup>. A single crystal grown by a miniaturized Bridgman technique could be cooled to  $-140^\circ\text{C}$ , however, preserved the pronounced disorder of the plastic crystal. The orientational disorder of the  $P_4$  molecules did not allow a convincing structure refinement.

Single crystals of  $\beta$ - $P_4$  could be grown from a solution in  $\text{CS}_2$  below  $-77^\circ\text{C}$ <sup>[12]</sup>. On the basis of data collected at  $-115^\circ\text{C}$  the structure was solved and refined in space group

$P\bar{1}$  yielding P–P distances between 215.8 and 218.0 pm, respectively. In spite of the low temperature of investigation the librational motion of the molecules was still very large. Correcting for libration resulted in P–P distances between 220.3 and 221.6 pm, as expected for single-bond lengths. The structure of  $\beta$ - $P_4$  (as that of  $\alpha$ - $P_4$ ) bears close similarities to yet another metal structure. The  $P_4$  molecules take the same positions as the metal atoms in the structure of  $\gamma$ -Pu<sup>[13]</sup>.

This paper concentrates on the following:

The  $\gamma$  modification is identified by X-ray powder diffraction, and experiments on single-crystal growth are reported. Phase relations between the different modifications are investigated, the structure of  $\beta$ - $P_4$  is redetermined at lowest accessible temperature and discussed in its relation to  $\gamma$ -Pu.

## Results and Discussion

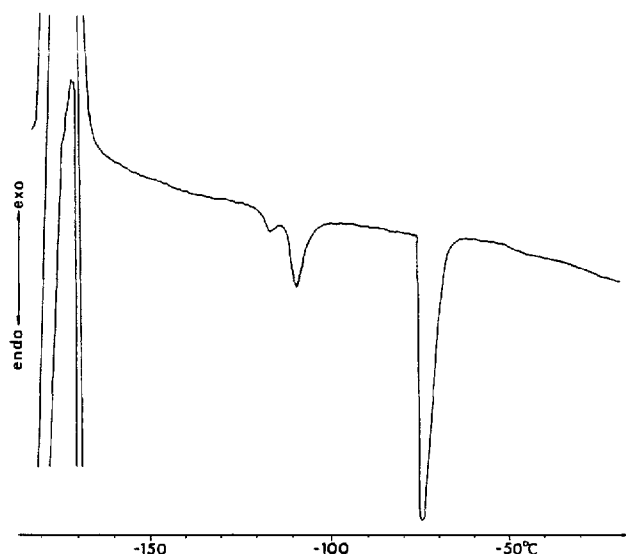
### a) Phase Transitions in White Phosphorus

When  $\alpha$ - $P_4$  is quenched in liquid nitrogen and slowly warmed, a number of thermal effects are observed. Figure 1 shows a typical record of a DTA investigation. At approx.  $-175^\circ\text{C}$  a very pronounced exothermic effect (I) occurs, followed by a weak endothermic one (II) at  $-119^\circ\text{C}$ , and immediately after that another endothermic effect (III) starts at  $-112^\circ\text{C}$ . The strong endothermic effect (IV) at  $-76.5^\circ\text{C}$  corresponds to the well-investigated  $\beta/\alpha$  transition. Effect II varies through different measurements and cannot be interpreted unambiguously.

The DTA measurements indicate that the supercooled  $\alpha$ -modification transforms into  $\gamma$ - $P_4$  with considerable evolution of heat.  $\gamma$ - $P_4$  is the stable<sup>[\*\*]</sup> low-temperature form and it transforms into the intermediate modification,  $\beta$ - $P_4$

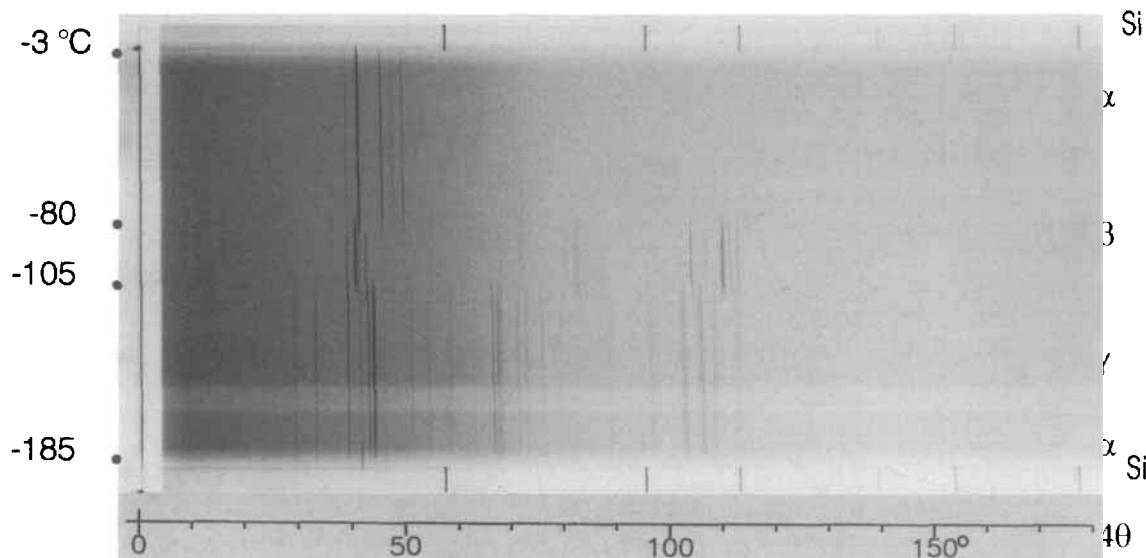
<sup>[\*]</sup> Here, the room-temperature modification is called  $\alpha$ , and the modification observed at lowest temperature is assigned  $\gamma$ .

Figure 1. DTA (5°C/min) of white phosphorus after quenching in liquid N<sub>2</sub>; the strong effect at -175°C corresponds to the transition of supercooled  $\alpha$ -P<sub>4</sub> to  $\gamma$ -P<sub>4</sub>, those between -120 and -110°C to the  $\gamma/\beta$  transition; the reason for splitting is unknown; at about -75°C the  $\beta/\alpha$  transition occurs



the modified Guinier technique<sup>[14]</sup>. Figure 2 shows a continuously recorded diffraction pattern of a sample quenched to -185°C. The diagram gives a first structural verification of the  $\gamma$ -modification. Its pattern changes with the formation of  $\beta$ -P<sub>4</sub>, slightly below -100°C. This pattern persists down to -185°C and changes into that of  $\alpha$ -P<sub>4</sub> upon warming. Repeated investigations of the  $\gamma/\beta$  transition led to some confusion as the X-ray powder pattern in the temperature range of  $\beta$ -P<sub>4</sub> was dramatically different from experiment to experiment. What could have appeared to be evidence for several other crystalline P<sub>4</sub> modifications turned out to be an artefact.  $\beta$ -P<sub>4</sub> forms from the  $\gamma$ -modification in surprisingly large crystallites. Therefore the powder diagram exhibits pronounced texture effects as seen in Figure 3. The X-ray diagram is recorded with 3 mm width on the continuously moving film, and contains a rather accidental intensity distribution. Besides these characteristics of the  $\beta$ -P<sub>4</sub> diagram the comparison of diagrams in Figure 2 shows another interesting feature: Whereas reflections can be observed up to large diffraction angles for  $\beta$ - and  $\gamma$ -P<sub>4</sub>, intensities quickly decrease in the case of  $\alpha$ -P<sub>4</sub>. This, together with the extremely sharp lines, is quite characteristic for a plastic crystal.

Figure 2.  $\Delta T$ -Guinier diagram of a shock-cooled sample of white phosphorus (Si at top and bottom); with rising temperature (1.2°C/h) supercooled  $\alpha$  form, changed to  $\gamma$ , to  $\beta$  and back to  $\alpha$ ; Cu-K<sub>α1</sub> radiation



stable between -112°C (-119°C) and -76.5°C, where it easily changes into  $\alpha$ -P<sub>4</sub> again. The phase transitions which reproducibly occur at rising temperature may be severely delayed or unobservable at decreasing temperature. As mentioned earlier, a single crystal of  $\alpha$ -P<sub>4</sub> could be cooled to -140°C without transforming into  $\beta$ -P<sub>4</sub>, and the transition of  $\beta$ -P<sub>4</sub> into  $\gamma$ -P<sub>4</sub> was never observed.

The results of thermal analyses are verified by temperature-dependent X-ray powder investigations performed with

#### b) Crystal-Growth Experiments with $\gamma$ -P<sub>4</sub>

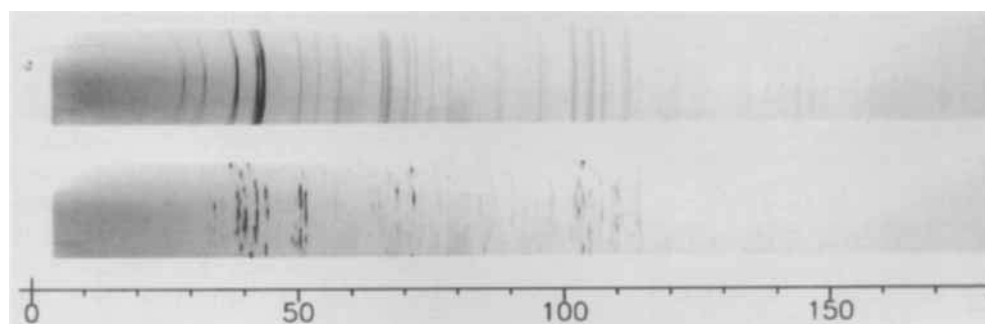
$\gamma$ -P<sub>4</sub> exhibits a characteristic powder pattern. Some lines are broadened which might be due to disorder in the structure or to accidental overlap of several closely spaced diffraction lines. We did not succeed in indexing the pattern<sup>[\*\*\*]</sup>. Therefore, crystal growth from suitable solvents below -125°C was tried.

As the solvent for white phosphorus, CS<sub>2</sub>, is solid in the stability range of  $\gamma$ -P<sub>4</sub>, solvent mixtures were tried which have a low enough melting point and yet should provide a

[\*\*] The term "stable" refers to the relative stabilities within the form of white phosphorus which, of course, is metastable with respect to red and black phosphorus.

[\*\*\*] Indexing was attempted with the program TREOR<sup>[15]</sup>.

Figure 3. Guinier diagram of  $\gamma$ -P<sub>4</sub> at  $-173^{\circ}\text{C}$  (top) and after change to  $\beta$  form at  $-115^{\circ}\text{C}$  (bottom) indicating severe recrystallization and very pronounced preferred orientation



sufficiently high solubility of phosphorus. Alkanes are quite efficient solvents for phosphorus, e.g. *n*-heptane which forms a 2.3 wt.-% solution at room temperature<sup>[16]</sup>. Finally, a mixture of 29 vol.-% methylcyclopentane in CS<sub>2</sub> was used which proved to be liquid down to  $-135^{\circ}\text{C}$ . Like the solution of  $\alpha$ -P<sub>4</sub> in CS<sub>2</sub>, the solution in the mixture also shows a miscibility gap (see c), and when cooled to  $-70^{\circ}\text{C}$  crystals of  $\alpha$ -P<sub>4</sub> are separating only from the P-rich and heavier phase. This was pipetted into an X-ray capillary and introduced as fast as possible into the cold gas stream set to  $-185^{\circ}\text{C}$  in the diffractometer. Polycrystalline  $\alpha$ -P<sub>4</sub> could be detected in addition to glassy solvent. The  $\alpha$ -P<sub>4</sub> transformed into  $\gamma$ -P<sub>4</sub> powder at  $-170^{\circ}\text{C}$ . Annealing between  $-130$  and  $-120^{\circ}\text{C}$  for one day, however, did not result in any detectable recrystallization. This behavior is in marked contrast to  $\beta$ -P<sub>4</sub>, which, even at  $-120^{\circ}\text{C}$ , grows to large single crystals. Single-crystal growth with  $\gamma$ -P<sub>4</sub> did not succeed. So its structure and the origin of the large difference in behavior of  $\beta$ - and  $\gamma$ -P<sub>4</sub> remains an open question.

### c) The Structure of $\beta$ -P<sub>4</sub>

The crystal structure of  $\beta$ -P<sub>4</sub> at  $-115^{\circ}\text{C}$  has briefly been reported<sup>[12]</sup>, however, no details on the crystal growth were mentioned. As the experimental procedure is widely applicable, it is described in the following. Crystal growth is performed below  $-77^{\circ}\text{C}$  from a saturated solution of  $\alpha$ -P<sub>4</sub> in CS<sub>2</sub> on a diffractometer. Problems are due to the miscibility gap mentioned previously, which occurs well above this temperature and leads to a separation into a heavier P-rich phase and a very dilute lighter one<sup>[17,18]</sup>. This phase separation can be utilized for a systematic crystal growth. The solution (saturated at room temperature) is contained in a sealed X-ray capillary to a height of approx. 20 mm. The capillary is surrounded by the cold gas stream of the diffractometer and kept in a vertical position. Lowering the temperature leads to the phase separation, and in the upper very dilute phase small crystallites of  $\beta$ -P<sub>4</sub> form below  $-77^{\circ}\text{C}$ . With the help of a removable metal screen kept at room temperature<sup>[19]</sup>, the phosphorus-rich phase is made to reach near a chosen  $\beta$ -P<sub>4</sub> crystallite which grows to a suitable single crystal within an hour. The single crystal used in the following was grown over night at  $-90^{\circ}\text{C}$  from the methylcyclopentane/CS<sub>2</sub> mixture (see b). To minimize the thermal motion of the P<sub>4</sub> molecules the crystal was meas-

ured at  $-185^{\circ}\text{C}$ . For that purpose the capillary with the crystal was quenched rapidly in order to avoid crystallization of the solvent and to reduce extinction effects.

Details of the data collection and structure refinement are summarized in the Experimental Section. Although the crystal slowly turned yellow-orange, the intensities of two check reflections only decreased by 3.6% during the total data-collection time of 186 h. The refinement on the basis of 4534 symmetry-independent reflections converged to  $wR2 = 0.053$ . Final positional and displacement parameters are summarized in Table 1, Tables 2 and 3 contain the bond lengths and bond angles, respectively.

Table 1. Fractional coordinates and displacement parameters [pm<sup>2</sup>] for  $\beta$ -P<sub>4</sub><sup>[a,b]</sup>

	<i>x</i>	<i>y</i>	<i>z</i>	<i>U</i> <sub>eq</sub>
P1	0.07292(6)	0.00036(3)	0.17674(3)	269.5(6)
P2	-0.16832(6)	-0.05448(3)	0.31113(3)	264.9(6)
P3	0.00612(7)	0.14473(3)	0.31184(3)	271.7(6)
P4	0.23909(6)	0.01003(3)	0.37323(3)	257.5(6)
P5	0.78223(6)	0.37474(3)	0.05849(3)	257.0(6)
P6	0.59210(6)	0.17605(3)	0.03117(3)	272.8(6)
P7	0.51082(7)	0.30715(4)	0.17458(3)	296.1(7)
P8	0.37938(6)	0.32142(3)	-0.02200(3)	270.1(6)
P9	0.31104(6)	0.68864(3)	0.47249(3)	256.3(6)
P10	-0.07263(5)	0.62577(3)	0.36581(3)	251.0(6)
P11	0.20456(6)	0.50517(3)	0.35888(3)	251.9(6)
P12	0.24277(6)	0.68078(3)	0.26975(3)	253.9(6)

<sup>[a]</sup> The anisotropic displacement factor exponent takes the form:  $-2\pi^2[(ha^*)^2U_{11} + \dots + 2hka^*b^*U_{12} - \dots]$ . <sup>[b]</sup>  $U_{eq}$  is defined as 1/3 of the trace of the orthogonalized  $U_{ij}$  tensor.

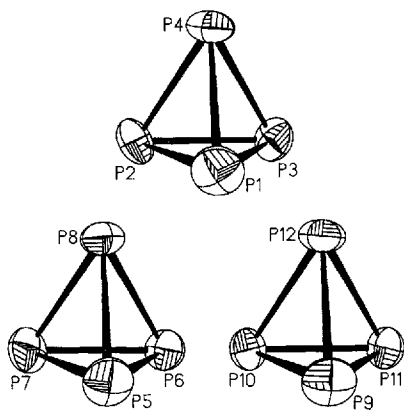
Table 2. Bond lengths [pm] for  $\beta$ -P<sub>4</sub> and the respective values after correction for librational motion (e. s. d.)

P1-P2	218.19(5)	220.4
P1-P3	219.10(5)	220.9
P1-P4	218.01(5)	220.4
P2-P3	218.28(5)	220.5
P2-P4	218.49(5)	220.6
P3-P4	217.68(5)	220.1
P5-P6	217.71(5)	220.1
P5-P7	217.56(5)	220.1
P5-P8	218.66(5)	220.7
P6-P7	219.20(5)	221.2
P6-P8	217.77(5)	219.9
P7-P8	218.08(5)	220.4
P9-P10	218.51(5)	220.7
P9-P11	218.34(5)	220.4
P9-P12	218.34(5)	220.3
P10-P11	218.18(5)	220.3
P10-P12	218.41(5)	220.3
P11-P12	218.74(5)	220.6

Table 3. Bond angles [°] for  $\beta$ -P<sub>4</sub>

P2–P1–P3	59.89(2)	P5–P7–P6	59.80(2)
P2–P1–P4	60.12(2)	P5–P7–P8	60.26(2)
P3–P1–P4	59.74(2)	P6–P7–P8	59.74(2)
P1–P2–P3	60.26(2)	P5–P8–P6	59.85(2)
P1–P2–P4	59.90(2)	P5–P8–P7	59.76(2)
P3–P2–P4	59.79(2)	P6–P8–P7	60.39(2)
P1–P3–P2	59.85(2)	P10–P9–P11	59.93(2)
P1–P3–P4	59.88(2)	P10–P9–P12	60.00(2)
P2–P3–P4	60.16(2)	P11–P9–P12	60.12(2)
P1–P4–P2	59.98(2)	P9–P10–P11	60.00(2)
P1–P4–P3	60.38(2)	P9–P10–P12	59.96(2)
P2–P4–P3	60.06(2)	P11–P10–P12	60.13(2)
P6–P5–P7	60.48(2)	P9–P11–P10	60.07(2)
P6–P5–P8	59.87(2)	P9–P11–P12	59.94(2)
P7–P5–P8	59.99(2)	P10–P11–P12	59.98(2)
P5–P6–P7	59.73(2)	P9–P12–P10	60.04(2)
P5–P6–P8	60.28(2)	P9–P12–P11	59.94(2)
P7–P6–P8	59.87(2)	P10–P12–P11	59.88(2)

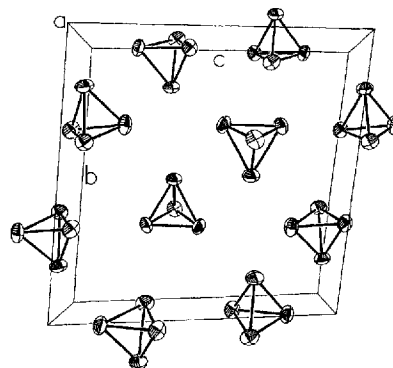
$\beta$ -P<sub>4</sub> crystallizes in space group  $P\bar{1}$  with three molecules in the asymmetric unit. The latter seems remarkable, as  $\alpha$ -P<sub>4</sub> adapts the  $\alpha$ -Mn structure with four crystallographically different P<sub>4</sub> molecules, while in the  $\beta$ -phase there are still three different molecules, although symmetry is dramatically reduced from cubic to triclinic. The independent molecules shown in Figure 4 exhibit only marginal deviations from symmetry  $T_d$ . The angles in the triangular faces range from 59.73 to 60.48° and the bond lengths (before libration correction) from 217.6 to 219.2 pm. In spite of the large difference between the temperature of measurement and the melting point of white phosphorus the molecules still exhibit large thermal motion at  $-185^\circ\text{C}$ . The isotropic displacement parameters (Table 1) lie between 251 and 296 pm<sup>2</sup>.

Figure 4. Three independent P<sub>4</sub> molecules in the  $\beta$  phase at  $-185^\circ\text{C}$ ; the ellipsoids are drawn at the 70-% probability level

As shown by Cruickshank<sup>[20]</sup>, and Busing and Levy<sup>[21]</sup> librational motion of molecules leads to (seemingly) shortened interatomic distances. These may be corrected by applying a rigid-body model<sup>[22]</sup>, which is based on the approximation that only translational and rotational motion of the whole molecule or a group of atoms occurs. The relevant parameters are determined from the anisotropic displacement parameters  $U_{ij}$  by least-squares refinements<sup>[23,24]</sup>. However, such refinements performed for (empty) tetrahedra result in singularities in the matrix of normal equations<sup>[25]</sup>. This problem can be overcome by in-

serting a “dummy atom” with isotropic displacement parameters at the centroid of the respective tetrahedron<sup>[26]</sup>. The libration analysis is performed in an iterative process. After one step of refinement the “dummy atom” is moved to the center which gave a symmetrical  $\hat{S}$  tensor, and its isotropic displacement parameter is recalculated from the anisotropic ones derived by the model. Throughout all rigid-body refinements the weight of the additional atom is set to 0.001. After three to four steps of iteration convergence was achieved with  $0.0028 \leq R \leq 0.0037$  for the agreement of observed to calculated displacement parameters for the three tetrahedra. The corrected P–P distances (Table 2) now lie between 219.0 and 221.2 pm. These distances are only slightly shorter than those, 222.28 pm<sup>[27]</sup>, determined by Raman spectroscopy for P<sub>4</sub> in the gas phase. For P<sub>2</sub>H<sub>4</sub> the value 222 pm has been given<sup>[28]</sup>. Thurn and Krebs determined the P–P distances in Hittorf’s phosphorus as 217.8–229.9 pm depending on the dihedral angles. Obviously, only the significant correction of bond lengths by applying the rigid-body model leads to reasonable values, although the corrections are extraordinary at 40 times the e. s. d. of a single P–P distance on average. This way another misinterpretation is avoided. Presuming each P atom was sp<sup>3</sup>-hybridized with a single-bond length of about 221 pm, the formation of tetrahedral P<sub>4</sub> molecules would lead to bent bonds with the direct P–P connection at about 218 pm<sup>[29]</sup>. This example clearly reveals how the inadequate description of a particular atomic motion in terms of an ellipsoid, as it is done in general crystal-structure refinement, may lead to a highly doubtful interpretation of the results.

A projection of the unit cell of  $\beta$ -P<sub>4</sub> is shown in Figure 5. The P<sub>4</sub> tetrahedra take rather irregular orientations in the crystal. Obviously an arrangement of tetrahedra, with a close-packing of atoms, as it is observed, e.g., in the close packing of Br atoms in SnBr<sub>4</sub><sup>[30]</sup>, is avoided.

Figure 5. Unit cell of  $\beta$ -P<sub>4</sub> projected down the  $a$  axis

To analyse the packing of tetrahedra in  $\beta$ -P<sub>4</sub> each molecule is substituted by a sphere. As seen in the projection of the structure along [001] in Figure 6, the spheres arrange in (buckled) layers formed from triangles and squares. Since each sphere belongs to three triangles and two squares, the net is of the kind 3<sup>3</sup>4<sup>2</sup>. Frank and Kasper<sup>[31]</sup> predicted a structure built of such nets with coordination number 14 for

Figure 6. Frank-Kasper-type arrangement of  $\beta$ -P<sub>4</sub>, each sphere representing one molecule; only two layers of the puckered 3<sup>3</sup>4<sup>2</sup> nets are shown for clarity

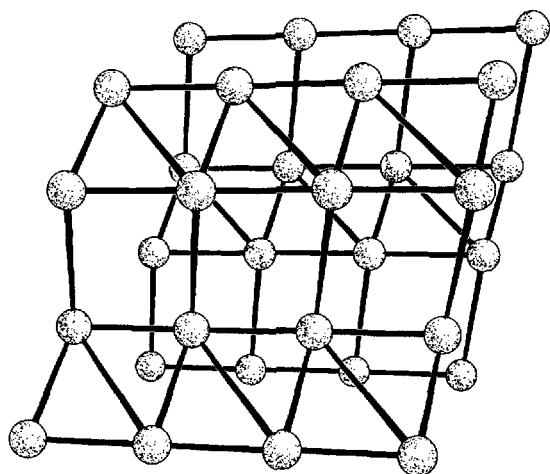
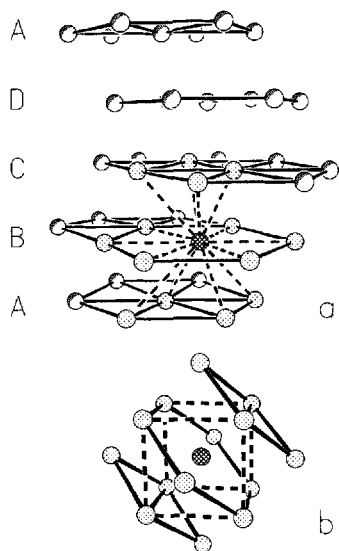


Figure 7. a) Sphere packing in  $\beta$ -P<sub>4</sub>; for simplicity each molecule is represented by a sphere; to emphasize the relation to the  $\gamma$ -Pu-type structure, one atom (cross-hatched) with its 14 nearest neighbors (dotted) is represented in a different way; the stacking sequence ABCDABCD... is also indicated; b) cubic body-centered arrangement showing the close relation to the  $\gamma$ -Pu-type as shown above



each atom, however, could not give an example at that time.

Another view of the structure is shown in Figure 7a. The spheres arrange in planar triangular nets which are stacked within the sequence ABCDABCD... along [011]. This sequence is not that of a close-packing of spheres, as each sphere does not lie above the center of a triangle in the adjacent layer, but above an edge. The arrangement is very similar to that of the atoms in  $\gamma$ -Pu. Each sphere has coordination number 14 which is reminiscent of the *bcc* lattice. Indeed, Figure 7b shows that the structural principle of  $\gamma$ -Pu is closely related to the *bcc* lattice. In the latter triangular nets are stacked along [110] in a way that the central atom lies above edges of triangles in adjacent layers, too. The difference lies in the fact that the indicated rhomboids coincide

in *bcc*, but show a relative rotation by 60° in the  $\gamma$ -Pu structure[\*\*\*\*].

The peculiar packing of tetrahedral molecules in  $\beta$ -P<sub>4</sub> raises an interesting question. Does the large difference between single-bond lengths and van-der-Waals distances between the P atoms simply obstruct against a close-packing? Or does the repulsive interaction between lone pairs of the P<sub>4</sub> molecule favor a structure with not too much interference between the lone pairs? In the latter case, the special electronic situation in  $\beta$ -P<sub>4</sub> might even mimic that in the actinide element plutonium and offer a clue to an understanding of the complicated structure in the  $\gamma$  modification of the metal.

## Experimental Section

**Preparation:** All handling was done in argon, purified with BTS catalyst<sup>[33]</sup> and Oxisorb<sup>[34]</sup>, in Schlenk tubes with seals and valves made from Teflon. Carbon disulfide (pro analysi, Merck) and methylcyclopentane (>99%, Janssen Chimica) were treated with molecular sieves (1-nm pores, Carl Roth GmbH) and distilled. White phosphorus was cleaned from oxide layers, washed with acetone and dried in a stream of argon. From then on, all operations were performed under red light. Phosphorus was sublimed in vacuum from +20 to -196°C and dissolved in a mixture of 29 vol.-% methylcyclopentane in CS<sub>2</sub>. The separating heavy phase was then pipetted into an X-ray capillary (0.2 mm diameter, 20 mm length) which was cooled and sealed with a hot platinum wire.

**DTA** was performed in a Heraeus DTA 500 apparatus using thin-walled glass ampoules (5 mm diameter, 50 mm length). The samples were quenched with liquid N<sub>2</sub>, introduced into the pre-cooled silver block and investigated with rising temperature.

**X-ray Powder Diffraction:** X-ray diagrams were recorded on capillary samples with a camera based on the modified Guinier technique<sup>[14]</sup> (temperature accuracy  $\pm 0.1^\circ\text{C}$ ; Cu-K $\alpha_1$ ,  $\lambda = 154.051$  pm, standard Si,  $a = 543.10$  pm<sup>[35]</sup>). Rapid cooling of the sample was achieved by quickly removing a piece of paper, which obstructed the gas stream from the sample until the determined temperature was reached.

**Single-Crystal Investigations:** Crystal growth was performed on a Syntex/Siemens P2<sub>1</sub> diffractometer equipped with a modified LT-1 low-temperature device (lowest temperature -185°C, accuracy  $\pm 2^\circ\text{C}$ , calibrated against ferroelectric transitions of AH<sub>2</sub>PO<sub>4</sub> and AH<sub>2</sub>AsO<sub>4</sub> with A = K, Rb, Cs, NH<sub>4</sub>). Crystallographic data:  $\beta$ -P<sub>4</sub> (123.88),  $a = 547.88(5)$ ,  $b = 1078.62(11)$ ,  $c = 1096.16(11)$  pm,  $\alpha = 94.285(8)$ ,  $\beta = 99.653(7)$ ,  $\gamma = 100.680^\circ$ ,  $V = 623.79(10) \cdot 10^6$  pm<sup>3</sup>,  $Z = 6$ ,  $d_{\text{calc}}$  = 1.979 g · cm<sup>-3</sup>, triclinic,  $P\bar{1}$  (no. 2), Mo-K $\alpha$  ( $\lambda = 71.069$  pm),  $\mu = 15.8$  cm<sup>-1</sup>, cylinder-like crystal  $d = 0.2$  mm,  $l \approx 0.3$  mm,  $T = -185 \pm 2^\circ\text{C}$ ,  $\omega/2\theta$  scans,  $4.0^\circ \leq 2\theta \leq 65.0^\circ$ , 4943 reflections measured, 4534 symmetry-independent, absorption correction based on  $\psi$  scans,  $T_{\text{min}} = 0.784$ ,  $T_{\text{max}} = 0.817$ , structure solution by Direct Methods, full-matrix least-squares refinement on  $F^2$ , 109 parameters,  $wR2 = 0.0531/R1 = 0.0242$  for all 4534 reflections. All calculations with SHELXTL-PLUS<sup>[36]</sup> and SHELXL-93<sup>[37]</sup> on a VAX-cluster. Libration correction was done with the programs XP (LIBR) and THMA-11<sup>[38]</sup>. Further details of the crystal structure investigation may be obtained from the

[\*\*\*\*] It is interesting to note that the  $\gamma$ -Pu structure was described as having  $cn = 10$  with neighbors at distances between 303 and 329 pm. It seems reasonable to include four more neighbors at 376 pm lying much closer than the next ones following at 491 pm<sup>[32]</sup>.

Fachinformationszentrum Karlsruhe, D-76344 Eggenstein-Leopoldshafen (Germany), on quoting the depository number CSD-406793.

\* Dedicated to Professor *Gottfried Huttner* on the occasion of his 60th birthday.

- [1] *Gmelins Handbuch der Anorganischen Chemie*, part B, system no. 16, Phosphor, 8th ed., Verlag Chemie, Weinheim, **1964**.
- [2] P. W. Bridgman, *J. Am. Chem. Soc.* **1914**, *36*, 1344–1363.
- [3] H. W. Spiess, R. Grosescu, U. Haeberlen, *Chem. Phys.* **1974**, *6*, 226–234.
- [4] H. Jung, *Zentralblatt Min. Geol.* **1926**, 107–115.
- [5] G. Natta, L. Passerini, *Nature* **1930**, *125*, 707–708.
- [6] T. Sugawara, E. Kanda, *Sci. Rep. Res. Inst. Tohoku Univ.* **1949**, *A1*, 153–155.
- [7] D. E. C. Corbridge, E. J. Lowe, *Nature* **1952**, *170*, 629.
- [8] J. Donohue, *The Structures of the Elements*, Wiley, New York, **1974**.
- [9] D. E. C. Corbridge, *The Structural Chemistry of Phosphorus*, Elsevier, Amsterdam, **1974**.
- [10] C. P. Gazzara, R. M. Middleton, R. J. Weiss, E. O. Hall, *Acta Crystallogr.* **1967**, *22*, 859–862.
- [11] H. G. v. Schnering, *Angew. Chem.* **1981**, *93*, 44–63; *Angew. Chem. Int. Ed. Engl.* **1981**, *20*, 33–52.
- [12] A. Simon, H. Borrmann, H. Craubner, *Phosphorus Sulfur* **1987**, *30*, 507–510.
- [13] W. H. Zachariasen, F. H. Ellinger, *Acta Crystallogr.* **1955**, *8*, 431–433.
- [14] A. Simon, *J. Appl. Crystallogr.* **1971**, *4*, 138–145.
- [15] P. E. Werner, L. Eriksson, M. Westdahl, *J. Appl. Crystallogr.* **1985**, *18*, 367–370.
- [16] K. Schäfer, E. Lax (ed.), *Landolt-Börnstein*, Teilband II/2b, 6th ed., Springer-Verlag, Berlin, Göttingen, Heidelberg, **1962**.
- [17] J. W. Retgers, *Z. Anorg. Chem.* **1894**, *5*, 211–230.
- [18] H. Giran, *J. Phys. Radium* **1903**, *2*, 807–809.
- [19] A. Simon, H.-J. Deiseroth, E. Westerbeck, B. Hillenkötter, *Z. Anorg. Allg. Chem.* **1976**, *423*, 203–211.
- [20] D. W. J. Cruickshank, *Acta Crystallogr.* **1956**, *9*, 757–758.
- [21] W. R. Busing, H. A. Levy, *Acta Crystallogr.* **1964**, *17*, 142–146.
- [22] J. D. Dunitz, E. F. Maverick, K. N. Trueblood, *Angew. Chem.* **1988**, *100*, 910–926; *Angew. Chem. Int. Ed. Engl.* **1988**, *27*, 880–895.
- [23] D. W. J. Cruickshank, *Acta Crystallogr.* **1956**, *9*, 754–756.
- [24] K. N. Trueblood, *Accurate Molecular Structures: their Determination and Importance*, Int. Union Crystallogr., Oxford University Press, Oxford, **1992**.
- [25] C. K. Johnson, *Computing in Crystallography*, the Indian Academy of Sciences for the Int. Union of Crystallogr., Bangalore, **1980**, 14.06.
- [26] H. Borrmann, Thesis, Stuttgart, **1988**.
- [27] N. J. Brassington, H. G. M. Edwards, D. A. Long, *J. Raman Spectr.* **1981**, *11*, 346–348.
- [28] H. Thurn, H. Krebs, *Acta Crystallogr.* **1969**, *B25*, 125–135.
- [29] H. G. v. Schnering, private communication.
- [30] P. Brand, M. Sackmann, *Acta Crystallogr.* **1963**, *16*, 446–451.
- [31] F. C. Frank, J. S. Kasper, *Acta Crystallogr.* **1958**, *11*, 184–190; *ibid.* **1959**, *12*, 483–499.
- [32] G. O. Brunner, *Acta Crystallogr.* **1977**, *A33*, 226–227.
- [33] M. Schütze, *Angew. Chem.* **1958**, *70*, 697–699.
- [34] H. L. Krauss, H. Stach, *Z. Anorg. Allg. Chem.* **1969**, *366*, 34–42.
- [35] P. Becker, P. Seyfried, H. Siegert, *Z. Phys.* **1982**, *B48*, 17–21.
- [36] G. M. Sheldrick, *SHELXTL-PLUS, Structure Determination Software*, Nicolet Instr. Corp., Madison, WI, **1990**.
- [37] G. M. Sheldrick, *SHELXL-93*, Göttingen, **1993**.
- [38] E. F. Maverick, K. N. Trueblood, *THMA-11 program*, Los Angeles, **1987**.

[97090]